ELSEVIER

Materials Science and Engineering A 435–436 (2006) 638–647

MATERIALS SCIENCE & ENGINEERING A

www.elsevier.com/locate/msea

Growth of intermetallic layer in multi-laminated Ti/Al diffusion couples

L. Xu, Y.Y. Cui, Y.L. Hao, R. Yang *

Shenyang National Laboratory for Materials Science, Institute of Metal Research, Chinese Academy of Sciences, Shenyang 110016, China

Received 10 April 2006; received in revised form 18 July 2006; accepted 18 July 2006

Abstract

Solid-state reactive diffusion between Ti and Al was investigated in the temperature range of 520–650 °C by employing multi-laminated Ti/Al diffusion couples. In samples annealed up to 150 h intermetallic $TiAl_3$ is the only phase observed in the diffusion zone and the preferential formation of this compound in Ti/Al diffusion couples was predicted using an effective heat of formation model. The present work indicated that both Ti and Al diffused into each other and the growth of the $TiAl_3$ layers occurred mainly towards the Al side. The $TiAl_3$ growth changes from parabolic to linear kinetics between 575 and 600 °C, characterized by activation energy of 33.2 and 295.8 kJ mol^{-1}, respectively. It is suggested that the low-temperature kinetics is dominated by the diffusion of Ti atoms along the grain boundaries of the $TiAl_3$ layers, while the reaction at the $TiAl_3$/Al interfaces in the high-temperature regime is limited by the diffusion of Ti atoms in the Al foils as a result of increased solubility of Ti in Al with increasing temperature.

Keywords: Growth behavior; $TiAl_3$ layer; Ti/Al diffusion couples; Phase prediction

抛物线

1. Introduction

Recently Ti–$TiAl_3$ metal–intermetallic laminate (MIL) composites have received growing attention because they have potential application in honeycomb or sandwich components of airplanes [1–3]. Ti–$TiAl_3$ MIL system can be more economical than monolithic titanium due to the use of relatively cheap aluminum foils in fabricating the composites. Of the available processing techniques, diffusion bonding of elemental titanium and aluminum foils is an effective low-temperature method to synthesize the composite, allowing growth of the intermetallic layer while both reactant materials (Ti and Al foils) are in the solid state [4]. So far Luo and Acoff [5,6] have used the technology to develop titanium aluminides by cold-roll bonding of multi-laminated Ti/Al foils followed by reactive diffusion above the melting point of aluminum. Most previous investigations however focused on the fabrication method of the composites and microstructural evolution of multilayered Ti/Al sheet. Few studies systemically dealt with mechanism and kinetics of the intermetallic layer growth during solid-state reaction and the reported data such as kinetic exponent and activation energy vary widely among different work in the temperature range of 500–640 °C [7–9].

The current understanding of diffusion process in the Ti–Al system is very incomplete. As far as interdiffusion is concerned the marker experiment conducted by van Loo and Rieck [7] suggested that Al is the only diffusing component in diffusion couples. Although this result was used to interpret $TiAl_3$ growth in several subsequent investigations [4,8], it should be noted that the marker experiment reported by van Loo and Rieck [7] was performed on a Ti–10 wt.% Al/Al diffusion couple and diffusion experiment using couples made from pure Ti gave "abnormal" result. On the other hand, Luo and Acoff [5] suggested that diffusion of Ti atoms to the Al side is much more pronounced than Al atoms to the Ti side.

In the present study, multi-laminated Ti/Al diffusion couples were prepared and annealing experiments were employed to identify the controlling mechanisms of the reactive diffusion at different temperatures in an attempt to clarify contradictions among previous reports.

2. Experimental procedure

Ti/Al laminates were prepared by stacking thin Ti (99.5%) and Al (99.5%) foils with titanium foils at both ends. The processed samples are 25 mm × 90 mm × 17 ply platelets. To

* Corresponding author. Tel.: +86 24 2389 3831; fax: +86 24 2389 1320.
E-mail address: ryang@imr.ac.cn (R. Yang).

0921-5093/$ – see front matter © 2006 Elsevier B.V. All rights reserved.
doi:10.1016/j.msea.2006.07.077

improve the condition of Ti/Al interfacial bonding, the Ti and Al foils were etched in 10% HF and 15% NaOH solution, respectively, alcohol cleaned, water flushed, and dried before stacking. Hot pressing was conducted at 600 °C for 3 h under 50 MPa, in a vacuum better than 10^{-2} Pa. The vacuum hot-pressed laminates were heat-treated in evacuated quartz tubes and then air-cooled. The thickness of the reaction layers at Ti/Al interfaces was measured from scanning electron microscope (SEM) micrographs of the cross-sections. For each condition, an average thickness was obtained from 20 individual measurements. Annealing experiments were carried out at 520, 550, 575, 600, 630 and 650 °C, with diffusion time varying from 1 h (3.6 ks) to 150 h (540 ks). An SEM equipped with energy dispersive X-ray spectrometer (EDS), an electron probe microanalyzer (EPMA) and an X-ray diffractometer (XRD) were used to identify intermetallic compounds formed during both vacuum hot-pressing and subsequent annealing treatments.

In addition to diffusion bonding, which was used to prepare samples for annealing experiment, cold-roll bonding and hot-roll bonding were both used to prepare samples for investigation of reaction mechanisms. In the former, stacked Ti/Al plies were rolled to 50% overall thickness reduction at room temperature; hot-roll bonding consisted of holding the stacked Ti/Al plies which were canned in 0.5 mm titanium foil to prevent oxidation and leakage of aluminum melt in furnace at 600, 750 and 950 °C for 5 min, and rolling the canned multilayers at a speed of 0.2 m/s to different ratios of thickness reduction.

3. Results

3.1. Phase identification

The vacuum hot-pressed laminates exhibited good bonding between the Ti and Al foils (with an average foil thickness of 175 ± 5 μm in the bonded condition). The interfaces between the bonded Ti and Al foils are fairly straight as can be seen from Fig. 1(a). At higher magnification, thin reaction layers with an average thickness of 2 μm can be observed (Fig. 1(b)). The thickness of the reaction layers increased remarkably when the annealing time and/or temperature were increased. Typical back-scattered electron (BSE) micrographs of the multilaminated diffusion couples annealed 12 h at different temperatures are shown in Fig. 2. EPMA analysis elucidated that the compositions of the grey, dark grey, and dark regions on each micrograph correspond to Ti, $TiAl_3$, and Al, respectively. An example of concentration profiles taken across a diffusion zone is shown in Fig. 3. The zone with roughly a composition of 75 at.% Al and 25 at.% Ti corresponds to $TiAl_3$ and no composition gradient can be noted within this zone. Formation of $TiAl_3$ was also confirmed by XRD analysis (Fig. 4), and further experiments suggested that in the temperature range of 520–650 °C $TiAl_3$ was the only compound observed after reactive diffusion between Ti and Al for time up to 150 h.

With increase in annealing time the Al foils were finally consumed and a Ti–$TiAl_3$ MIL composite was obtained. During second-stage annealing at higher temperatures, e.g. 700 °C/1 h + 800 °C/1 h, a thin layer (~2 μm) of TiAl phase

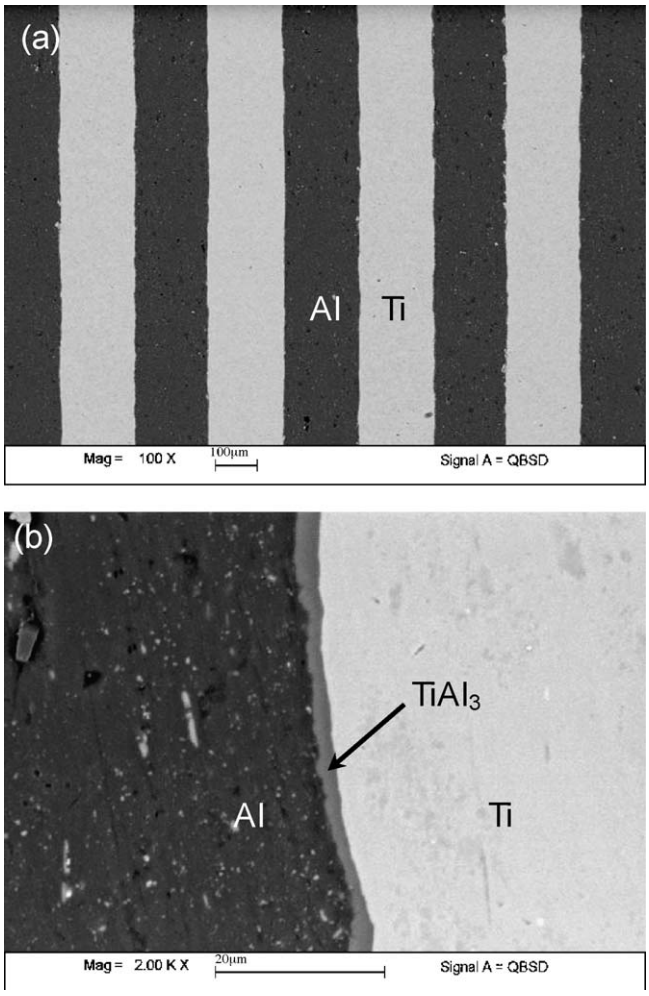

Fig. 1. (a) SEM micrograph showing morphology of a Ti/Al laminate after hot-press bonding at 600 °C for 3 h. (b) The Ti and Al layers have equal thickness of ~175 μm and a thin layer (with an average thickness of 2 μm) of $TiAl_3$ is present at the interface.

formed between the Ti and $TiAl_3$ layers (Fig. 5). The composition of this newly formed phase obtained by EDS analysis on SEM is listed in Table 1. The average composition of 51.2 at.% Ti and 48.8 at.% Al corresponds to that of the TiAl phase.

3.2. Morphological observation

In order to understand how $TiAl_3$ formed, both the diffusion bonded and cold- or hot-roll bonded samples were investigated. In the hot-roll bonded samples, metallography of the Ti foil sections close to the Ti/$TiAl_3$ interfaces shows the presence of

Table 1
Composition (in at.%) of the second phase formed at the Ti/$TiAl_3$ interface

Position	Al content	Phase
1	44.88	TiAl
2	46.76	TiAl
3	52.98	TiAl
4	50.64	TiAl

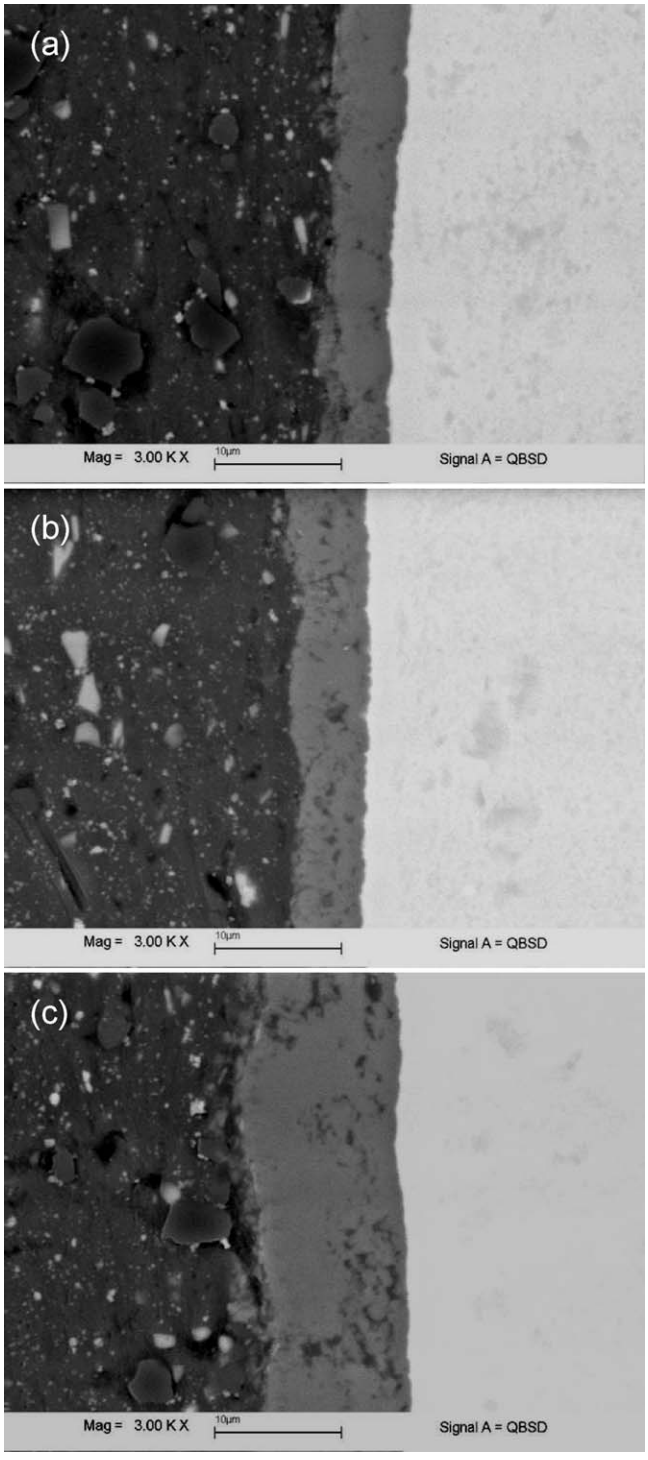

Fig. 2. BSE images of the interface region of samples annealed for 12 h in vacuum at 550 °C (a), 575 °C (b), and 600 °C (c).

globular particles of $TiAl_3$ along the Ti grain boundaries after annealing (Fig. 6(a)), providing evidence of the diffusion of Al atoms along these grain boundaries. Because the Al foils were consumed faster than Ti foils and because of the formation of voids and cracks in the Al/$TiAl_3$ interface regions, attempts to make similar observation on the grain boundaries of the Al foils failed. An observation of the fracture surface of a $TiAl_3$ layer revealed fine, globular grains of this intermetallic phase

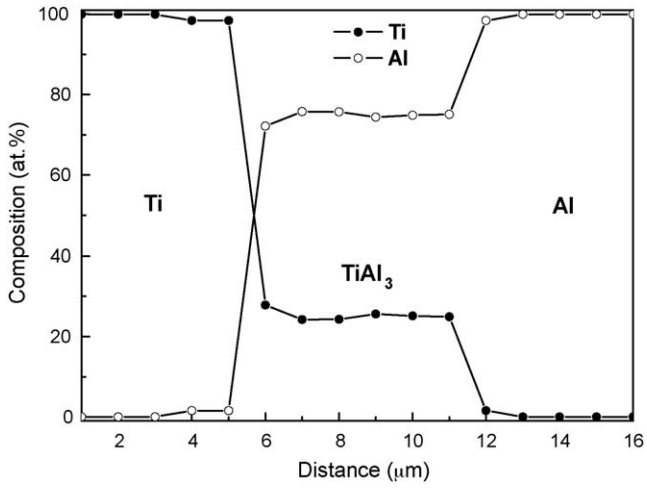

Fig. 3. Concentration profiles across the diffusion zone of a laminate.

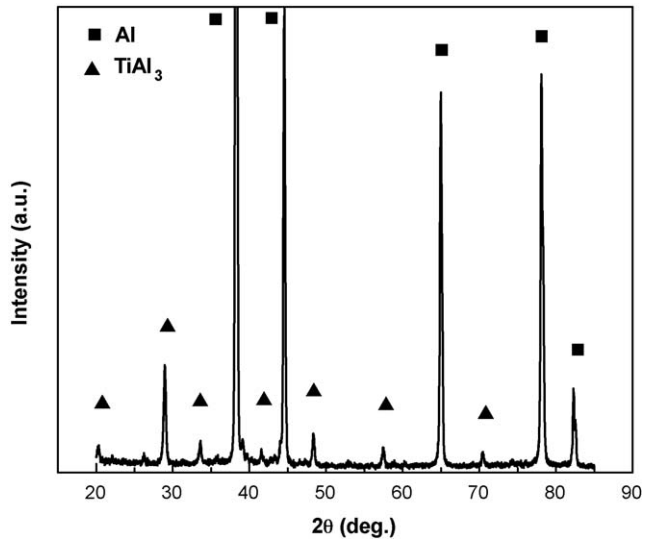

Fig. 4. XRD pattern of the reaction zone of a Ti/Al laminate annealed at 630 °C for 4 h (from the Al side of the interface).

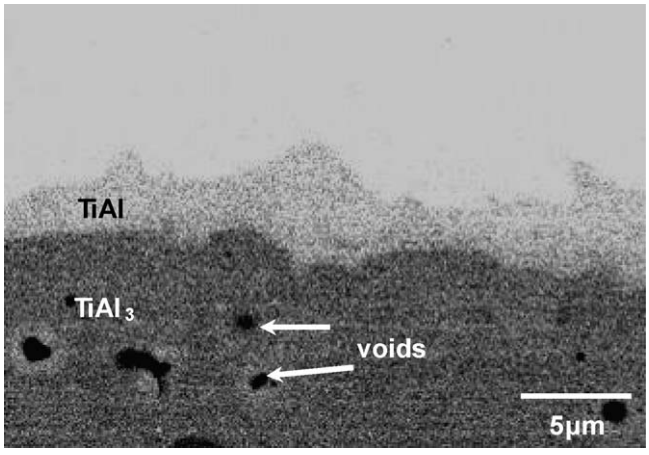

Fig. 5. SEM secondary electron image of the Ti–$TiAl_3$ MIL composite after a second-stage annealing of 700 °C/1 h + 800 °C/1 h. TiAl formed at the interface between Ti and $TiAl_3$.

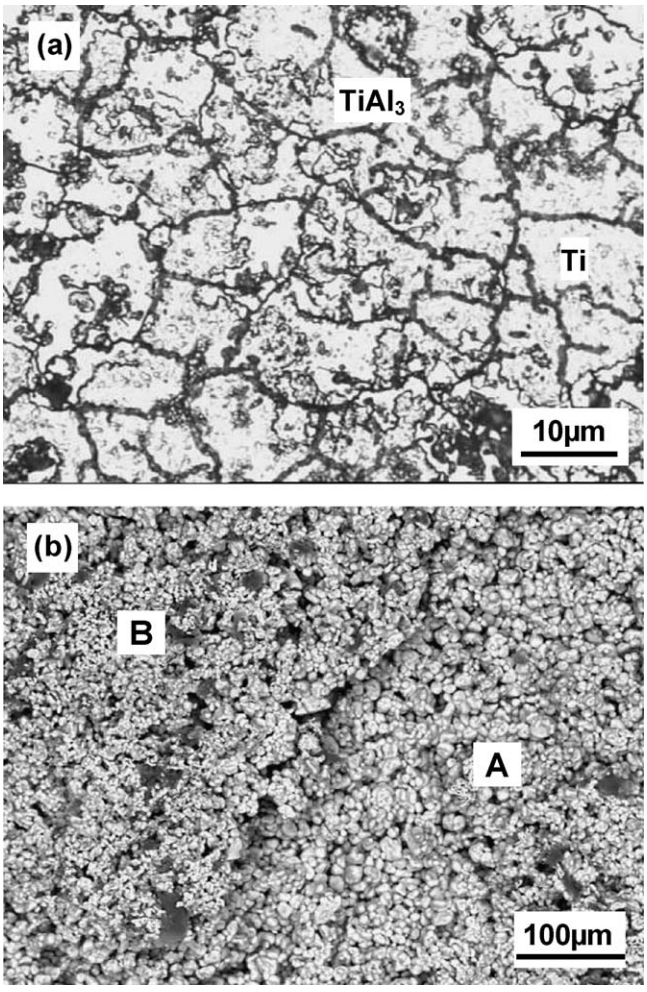

Fig. 6. Planar view of Ti foil close to a Ti/$TiAl_3$ interface (a, optical micrograph) showing formation of $TiAl_3$ at grain boundaries of a Ti foil, and intergranular fracture surface of a cracked $TiAl_3$ layer (b, SEM) showing fine globular grains of $TiAl_3$. Grain size in region A is larger than that in region B. Samples were hot-roll bonded at 600 °C followed by annealing at the same temperature for (a) 5 h and (b) 15 h.

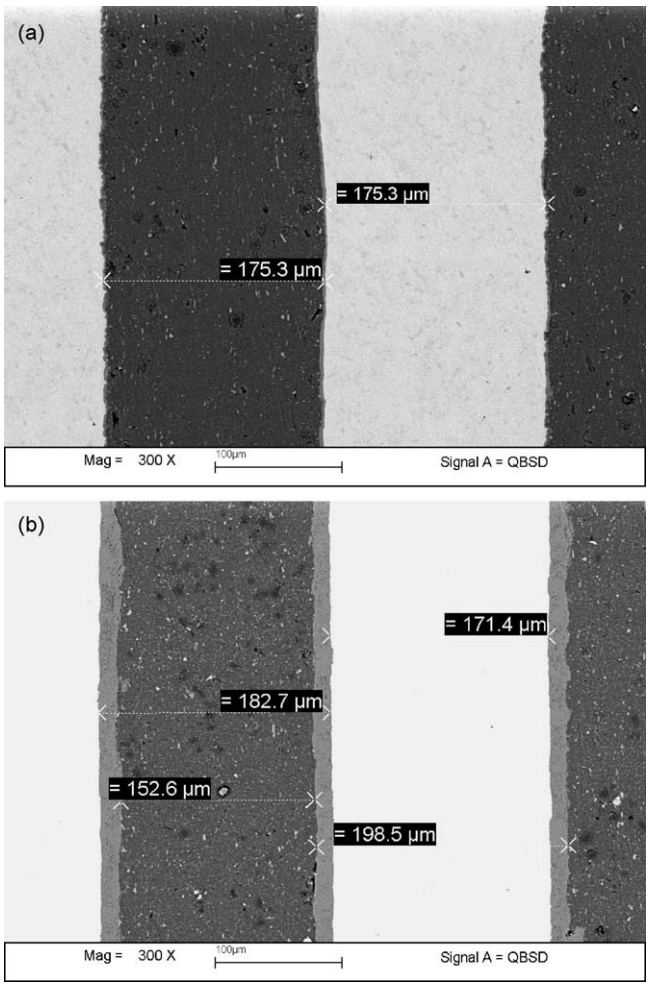

Fig. 7. SEM micrographs from which layer thickness was measured: (a) as hot-press bonded sample; (b) sample annealed at 575 °C for 63.5 h, in which the Ti, Al and $TiAl_3$ layer thickness becomes 171.4, 152.6 and 14.3 μm, respectively.

(Fig. 6(b)). This fracture surface, however, appears terraced (阶梯状的) and the particle size in region A is larger than that in region B.

To help clarify the characteristics of diffusion, positions of the interfaces during the growth of $TiAl_3$ were carefully determined on cross-sections of laminate samples with equal starting thickness of Ti and Al foils. Fig. 7(a) and (b) compare an as-bonded sample with one subjected to an anneal of 63.5 h at 575 °C: the thickness of the Ti foils shrinked only slightly by ~3.9 μm during annealing whereas the thickness of the Al foils reduced by ~22.7 μm. Clearly the growth of $TiAl_3$ occurred mainly on the Al foil side of the interface. The present result, consistent with that of Luo and Acoff [5], indicates that Ti atoms also diffuse into the Al foils.

The observation of Fig. 6(a) suggests that grain boundaries are important diffusion channels during Ti/Al interdiffusion. With increase in $TiAl_3$ layer thickness the diffusion of Ti and Al into each other must penetrate the intermetallic layers, and the observation of fine-grain structure of the $TiAl_3$ layer (Fig. 6(b)) suggests that grain-boundary mechanism is also important in this process. It is also known that other crystal defects such as dislocations provide extra diffusion channels. To verify this mechanism, samples subjected to different amount of plastic deformation during hot-roll bonding at 600 °C were annealed for identical time of 5 h (see Fig. 8). Measurement indeed showed that the average layer thickness increased with the amount of rolling reduction, suggesting that the increased density of dislocations in both Al and Ti foils is beneficial to subsequent diffusion.

3.3. Intermetallic layer thickening

The average thickness values of the $TiAl_3$ layers after annealing at different time and temperature are collected in Table 2. Although annealing experiments up to 150 h have been performed, the irregular interface profile at long annealing time makes accurate measurement of the layer thickness impossible, especially at high temperatures. As a result, the layer thickness data for temperatures above 600 °C are limited to short annealing time.

It is worth noting that the layer thickness data given in Table 2 suggest that growth kinetics at 520 and 550 °C are quite similar

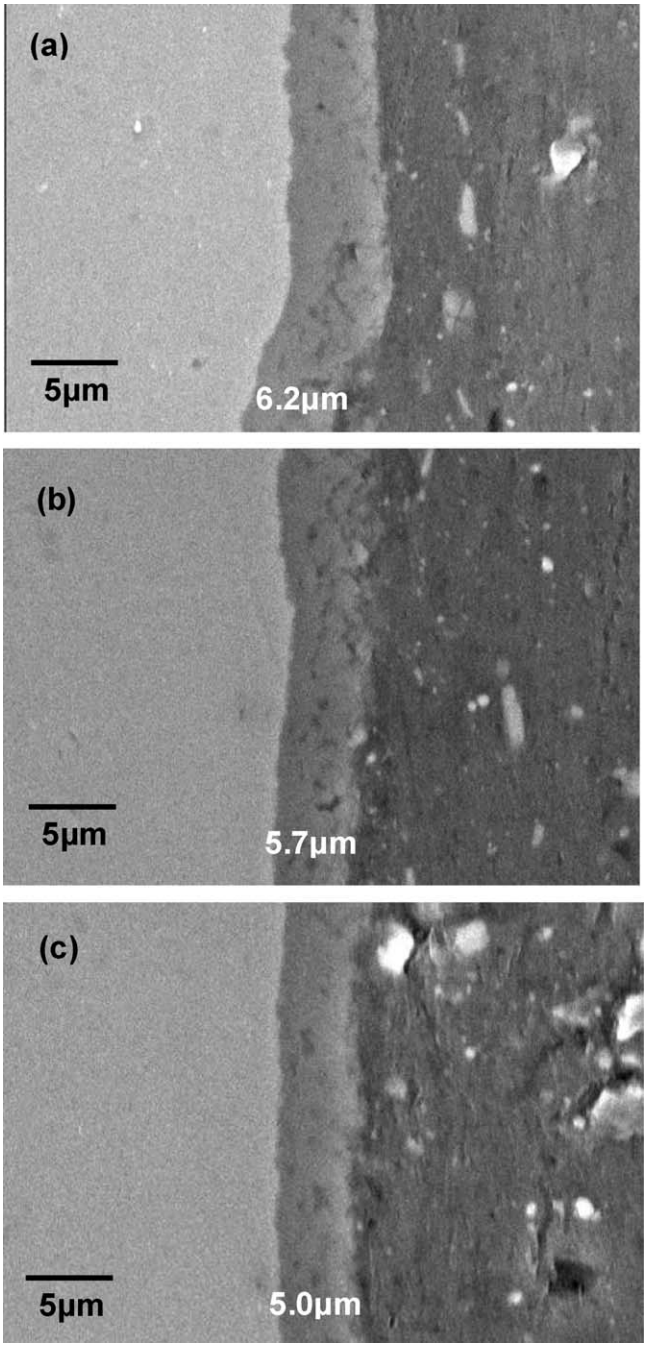

Fig. 8. SEM images of samples prepared by hot-rolling at 600 °C to overall thickness reduction of (a) 73%, (b) 61%, and (c) 51%, followed by annealing for 5 h at the same temperature. The average thickness of the $TiAl_3$ layer under each condition is indicated on the photographs.

if the errors of measurement are considered. The mean thickness values for 550 °C at identical annealing time are even slightly less than those for 520 °C.

It is well known [10] that at a given temperature the dependence of the thickness of an interdiffusion layer on diffusion time can be described by the following empirical relationship:

$$\Delta x = kt^n \quad (1)$$

$$\ln \Delta x = n \ln t + \ln k \quad (2)$$

Table 2
Experimental data of average $TiAl_3$ layer thickness Δx (after deduction of the starting thickness of 2 μm) at different time (t) and temperature (T)

T (°C)	t (h)	Δx (μm)
520	2	1.02 ± 0.34
	6	2.08 ± 0.40
	12	4.46 ± 0.61
	43	5.14 ± 0.78
	48	6.38 ± 0.77
	64	10.50 ± 0.78
550	2	0.88 ± 0.40
	6	2.04 ± 0.40
	13	3.52 ± 0.61
	40	4.15 ± 0.78
	48	5.74 ± 0.77
	64	6.58 ± 0.78
575	2	1.02 ± 0.46
	6	2.06 ± 0.34
	12	4.45 ± 0.36
	20	5.15 ± 0.96
	43	6.36 ± 0.74
	63.5	10.45 ± 1.31
600	2	1.15 ± 0.75
	3	1.80 ± 0.48
	5	2.88 ± 0.62
	6	3.60 ± 0.63
	12	5.89 ± 0.78
630	2	9.58 ± 1.16
	3	15.30 ± 1.75
	5	26.50 ± 0.99
	6	31.20 ± 0.99
	12	66.85 ± 1.59
650	1	4.00 ± 0.75
	2	11.04 ± 1.06
	3	17.06 ± 2.00
	4	24.11 ± 5.85

where Δx is the thickness of the reaction layer, k the rate constant, t the diffusion time, and n is the kinetic exponent. The values of pairs of Δx and t at different temperatures measured in the present work as listed in Table 2 were substituted into Eq. (2) and six plots of $\ln \Delta x$ versus $\ln t$ were obtained and shown in Fig. 9(a). Linear regression analysis gives six best-fit straight lines, with values of the kinetic exponent n of 0.55, 0.49, 0.47, 0.83, 1.08 and 1.06 for the temperatures of 520, 550, 575, 600, 630 and 650 °C, respectively. An n value of 0.5 suggests standard diffusion limited growth and $n > 0.5$ indicates interface-controlled growth. Taking into account the experimental errors, it is reasonable and convenient to divide the present data into two groups, each with three temperatures, and to assume n values of 0.5 and 1.0 for the two groups (as plotted in Fig. 9(b)).

The activation energy for both diffusion-controlled and reaction-controlled growth can be obtained from the rate constant k, which is usually assumed to follow an Arrhenius-type relation at different temperature:

$$k = A \exp\left(-\frac{E_a}{RT}\right) \quad (3)$$

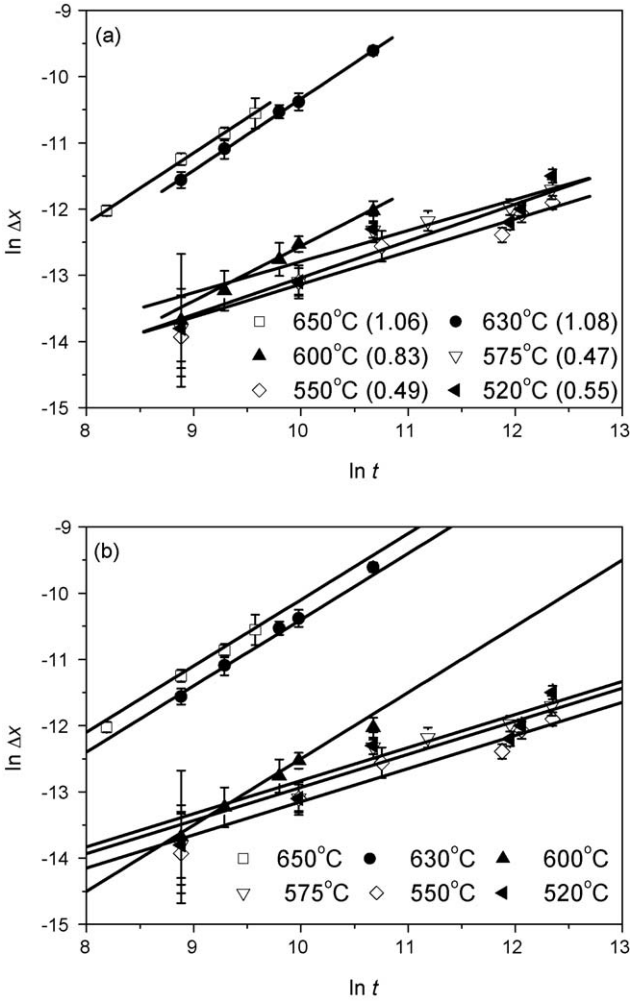

Fig. 9. (a) Plots of $\ln \Delta x$ vs. $\ln t$ by linear regression analysis using Eq. (2) with the values of n in the parentheses. (b) Re-plots of the data by assuming $n = 0.5$ (520, 550 and 575 °C) and $n = 1.0$ (600, 630 and 650 °C).

where A is the pre-exponential factor, E_a the activation energy for growth, R the gas constant, and T is the absolute temperature. Eq. (3) can also be written in the following form:

$$\ln k = \ln A - \frac{E_a}{RT} \quad (4)$$

The activation energy can be obtained from plots of $\ln k$ versus the reciprocal of temperature. Such plots are given in Fig. 10, yielding activation energies of 33.2 and 295.8 kJ mol^{-1} for the two groups with n values of 0.5 and 1.0, respectively. The respective values of A in the two cases are 2.1×10^{-6} m s$^{-0.5}$ and 1.2×10^{8} m s^{-1}.

4. Discussion

4.1. Sequence of phase formation

Annealing in the temperature range of 520–650 °C in the present study resulted in the formation of only one phase, $TiAl_3$, even though the phase diagram suggests other compounds, such as Ti_3Al, TiAl and $TiAl_2$, should also be formed between Al and

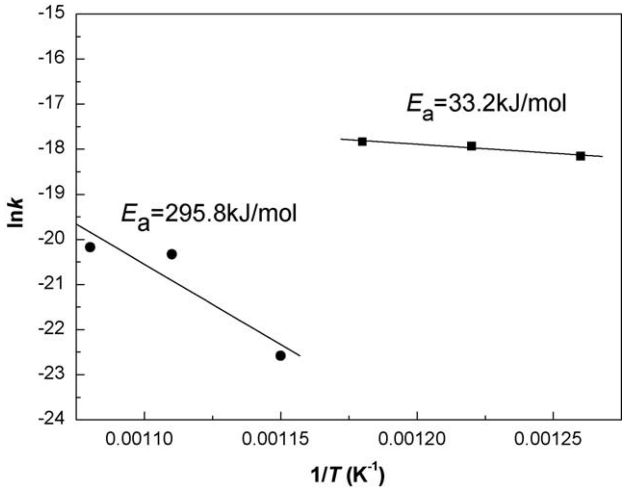

Fig. 10. Plots of the rate constant k for $TiAl_3$ layer growth against temperature for the two mechanisms.

Ti in the diffusion process. The absence of these compounds in the Ti/Al diffusion couples was also noted by previous investigators [7,11–13], who attributed the absence of phases other than $TiAl_3$ to the much faster diffusion in $TiAl_3$ than in other intermetallic phases of the Ti–Al system. van Loo and Rieck [7] prepared a Ti–Ti_3Al–TiAl–$TiAl_2$–$TiAl_3$–Al diffusion system and annealed it at 625 °C for 15 h. They found that the interjacent layers with a total thickness of 12 μm vanished completely and the system changed to Ti–$TiAl_3$–Al. This experiment proved that difficulties in nucleation of one of the interjacent phases could not be the cause of its absence in the diffusion couples.

In general, the sequence of intermetallic phase formation is determined by not only the thermodynamics but also the diffusion kinetics of the system concerned. In the Ti–Al binary system, several intermetallic compounds appear as equilibrium phases: $TiAl_3$, Ti_2Al_5, $TiAl_2$, TiAl, and Ti_3Al. Of these the formation of Ti_2Al_5 and $TiAl_2$ necessarily involves TiAl as one of the starting phase [14], and so may be omitted in our consideration here. Plots of the free energy of formation of the intermetallic phases with temperature [15], as done by Peng et al. [3], suggested that above ~500 °C Ti_3Al should be the second phase to form following $TiAl_3$ since Ti_3Al has more negative free energy than TiAl. This does not agree with the experimental observation that TiAl is the second phase to appear between Ti and $TiAl_3$ (see Fig. 5). Clearly, kinetic influences must be taken into account in theoretical models in order to make correct predictions.

There have been many attempts at establishing models for predicting first phase formation in a binary system [16–18]. The effective heat of formation (EHF) model proposed by Pretorius et al. [19,20] was the most recent and it succeeded in predicting the formation of first phase in 15 metal–aluminum binary systems. However, in some systems where congruent and non-congruent compounds were simultaneously present, the EHF model encountered difficulty. To resolve this issue a modified effective heat of formation (MEHF) model was recently proposed by Kale and co-workers [21] who incorporated a con-

Table 3
The values of ΔH° [18] and ΔH^m for various intermediate phases in the Ti–Al system

Phase	Compound concentration	ΔH°, kJ (mol at.)$^{-1}$	Limiting element	ΔH^m, kJ (mol at.)$^{-1}$
Ti_3Al(NC[a])	$Ti_{0.750}Al_{0.250}$	−25	Ti	−0.67
TiAl(NC)	$Ti_{0.500}Al_{0.500}$	−38	Ti	−1.52
$TiAl_3$(NC)	$Ti_{0.250}Al_{0.750}$	−37	Ti	−2.96

[a] NC, non-congruent.

gruency factor, ΔH^f, into the original formulation of Pretorius et al. and rewrote the effective heat of formation as:

$$\Delta H^m = (\Delta H^\circ + \Delta H^f)\frac{C_e}{C_l} \quad (5)$$

where ΔH° is the standard heat of formation, C_e the effective concentration of the limiting element at the interface, taken as the concentration of the limiting element at the lowest liquidus temperature, and C_l is the concentration of the limiting element in the compound. These authors demonstrated that this model works well for the Zr–Al system [21]. For the Ti–Al binary system the concentration at the lowest liquidus temperature was $Ti_{0.020}Al_{0.980}$ (see Ti–Al binary diagram [22]); obviously Ti is the limiting element for all the titanium aluminides, which may form at the Ti/Al interface. Here ΔH^f is assumed equal to the heat of crystallization for congruent compounds and zero for non-congruent compounds formed at the interface. The congruency factor can be empirically 经验主义 related to the melting point T_m of the intermediate phase by the relation [21]: $\Delta H^f = 8.13T_m$ J mol^{-1}. Because all intermetallic compounds in the Ti–Al binary system are non-congruent, the values of ΔH^f are zero. The values of ΔH^m were calculated for the candidate compounds taken from the phase diagram and are listed in Table 3 along with the values of ΔH°. Clearly $TiAl_3$ has the most negative effective heat of formation (ΔH^m), and is expected to be the first phase to form in the diffusion zone, in agreement with experimental observations.

Pretorius [19,20] predicted that after the formation of the first phase in a metal–metal binary system, the next phase to form at the interface between the compound phase and the remaining element is the next phase that has the most negative effective heat of formation. In Ti–Al binary system the second phase to form in the diffusion zone is predicted to be TiAl (see Table 3), in agreement with experimental observations (Fig. 5). Yang and Weatherly [23] suggested that TiAl formed first between $TiAl_3$ and Ti layers due to the reaction of $TiAl_3 + Ti \rightarrow 3TiAl + \Delta H$. The above theoretical prediction based on the MEHF model is also consistent with the experimental results of Luo and Acoff [5,6].

4.2. Interdiffusion in Ti–Al system

Al is commonly regarded as the only diffusing species in the Ti–Al system below its melting point (660 °C) and growth of $TiAl_3$ was thought to occur only on the Ti-rich side [7,24,25]. Above the melting point of Al, Ti was shown to be the diffusing species [26,27]. As noted by previous authors [2,7] many factors such as failure to remove surface oxide film may modify the diffusion behavior. In the present work, diffusion of both Ti and Al into each other was observed at all temperatures. In their recent study of thin-film interdiffusion, Ramana et al. [28] observed significant diffusion of Ti atoms into Al single crystals on the (1 1 0) surface above 400 °C, and on the (1 0 0) and (1 1 1) surfaces of Al crystals above 452 °C. Although the formation of $TiAl_3$ is an exothermic 放热的 reaction and this may cause a temperature rise, it is not sufficient to melt Al at most annealing temperatures employed in the present study. In Al melt, diffusion of Ti atoms is accelerated and the globular $TiAl_3$ particles formed are decorated by a thin layers of Al, as can be seen from Fig. 11. In the absence of pressure voids and cracks may form near the mid-planes of original Al foils after the Al melt is consumed completely (Fig. 12). This suggested that Al atoms also diffuse across the $TiAl_3$ layers to react with Ti at the Ti/$TiAl_3$ interfaces, and the rugged appearance of these interfaces seen in Fig. 12 is an indication of growth front. From the above discussion it can be concluded that both Ti and Al are diffusing species in the binary system regardless of the temperature being above or below the melting point of Al.

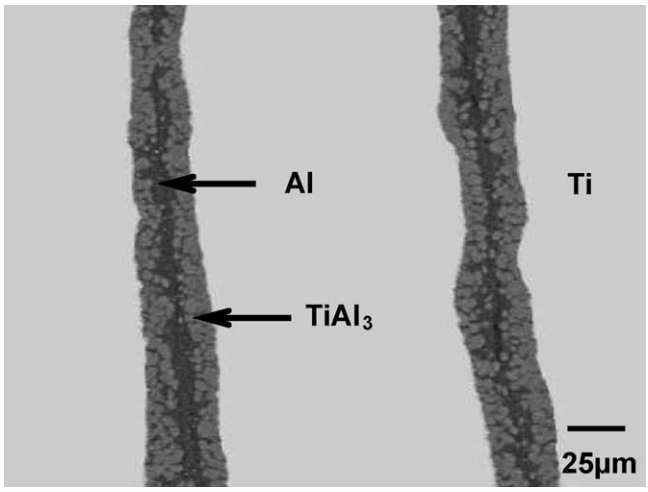

Fig. 11. Optical micrograph of a Ti/Al laminate held at 750 °C for 5 min and then hot-rolled to 48% thickness reduction.

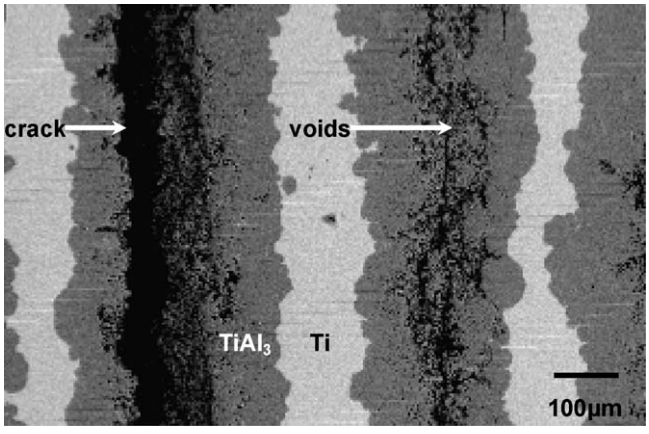

Fig. 12. SEM micrograph of a cold-roll bonded laminate annealed at 660 °C for 4 h.

4.3. Kinetics of $TiAl_3$ growth

As discussed in Section 4.1, kinetically $TiAl_3$ is expected to form first at the Ti/Al interfaces during annealing. The kinetics of diffusion also determines to which side the $TiAl_3$ layers grow faster. According to the Ti–Al binary phase diagram [22], the terminal solution Al(Ti) has a very narrow domain of existence, whereas the solid solution Ti(Al) exists over a wide composition range. In the temperature range studied in this work (520–650 °C), the solubility of Al in Ti is ~11.7 at.%, whereas the maximum solubility of Ti in Al is about two orders of magnitude smaller, only ~0.12 at.% [29]. One would expect the Al(Ti) solid solution to saturate much earlier than the Ti(Al) in nucleating $TiAl_3$ (considering the fact that the solubility of 11.7 at.% is for Ti_3Al rather than $TiAl_3$ lends still stronger support for the above argument). Another factor to consider is the stoichiometry of the product phase, which consists of 1 part Ti and 3 parts Al. Even if the solubility is similar on both sides of the intermetallic layers, an equal flux of Ti and Al atoms across the layers would result in growth rate on the Al foil side to be three times that on the Ti foil side if nucleation rate of $TiAl_3$ is similar on both sides.

With the growth of the $TiAl_3$ layers Ti and Al atoms must diffuse through the layers before reactions at the Ti/$TiAl_3$ and the $TiAl_3$/Al interfaces proceed. A schematic of the reactive diffusion process is shown in Fig. 13(a). The Ti(Al) solid solution region is drawn much larger than the Al(Ti) region to illustrate different solubility. Similarly, the density of $TiAl_3$ nuclei (reflecting layer thickening rate) is different on both sides of the $TiAl_3$ layer. We expect the distribution of $TiAl_3$ nuclei on the Al side to be much more uniform due to very limited solubility; on the Ti side, $TiAl_3$ nuclei may form at the grain boundaries of the Ti foils (which provide fast diffusion channels for the Al atoms) when the solubility is locally exceeded. van Loo and Rieck [7] suggested that grain-boundary diffusion is the dominant mechanism in the mass transport through the $TiAl_3$ layers in Ti/Al reactive diffusion system. In the present experiment observation of fine grains of the $TiAl_3$ layers (see Fig. 6(b)) supports such an argument.

If a growth process is limited by lattice diffusion, parabolic growth behavior is expected and the kinetic exponent will be $n = 0.5$. If grain boundary diffusion is significant, the situation is much more complex, because the grains grow with the increase of both annealing time and temperature. As illustrated in Fig. 13(b), there is a distribution of grain size, which is difficult to describe accurately. The observation of different grain size on a terraced fracture surface (see Fig. 6(b), regions A and B) confirmed the variation of grain size with depth within a layer. The largest grain size occurs at the initial Ti/Al interfaces, and in the present case this is close to the Ti/$TiAl_3$ interfaces because growth of the intermetallic layers occurs mostly towards the Al foils. With increase in annealing temperature and time, grain growth or Oswald ripening reduces the effectiveness of grain-boundary diffusion [30,31]. Many simplified treatments of grain-boundary diffusion (e.g. [32,33]) suggested a kinetic exponent close to $n = 1/3$. In general, the values of n will vary between 0.25 and 0.5 [34]. If the grain size is small compared

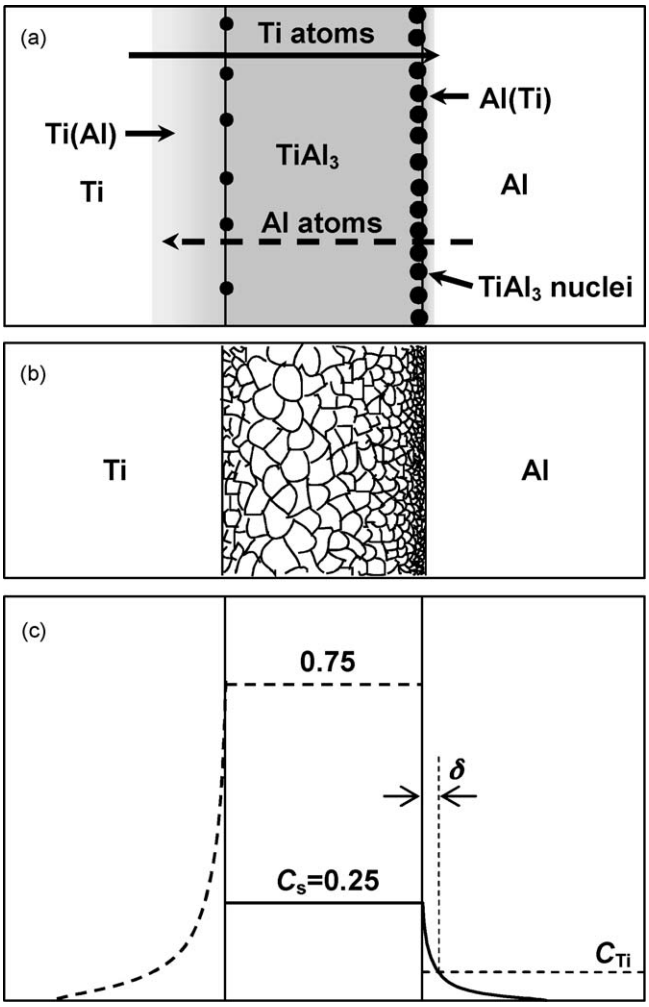

Fig. 13. Schematic illustration of Ti/Al reactive diffusion process. The diffusion of Ti into Al and vice versa are indicated by solid and dash arrows in (a), and their concentration profiles are represented by solid and dash lines in (c). $TiAl_3$ nuclei, with different growth rate at the Ti/$TiAl_3$ and $TiAl_3$/Al interfaces, are represented by dots of different density, and the different solubility of Ti in Al and Al in Ti is illustrated by different width of the shaded region in (a). The grain size distribution within the $TiAl_3$ layer as a result of grain growth is schematically shown in (b).

to the thickness of the intermetallic layer, however, parabolic growth law will hold even if grain-boundary diffusion dominates [34]. Because $TiAl_3$ is a line compound that dissolves neither Ti or Al during diffusion, as evidenced by the concentration profile of the intermetallic layer (Fig. 3), the diffusing atoms of both Ti and Al are confined to the grain boundary regions. Such a high concentration of moving atoms at grain boundaries behaves like a second phase and slows down grain growth. This has two consequences: (a) the domination of grain boundary diffusion will persist to relatively higher temperatures than usual; (b) the condition for $n = 0.5$, that is, grain size is small compared to $TiAl_3$ layer thickness, will be satisfied for a wider temperature range. Growth data obtained in the present work between 520 and 575 °C, with an approximate kinetic exponent of 0.5 (Fig. 9), is in support of the above argument. The low activation energy of 33.2 kJ mol^{-1} is in accord with the assumption of grain-boundary diffusion. An activation energy of 34 kJ mol^{-1}

Table 4
Comparison of different studies of $TiAl_3$ growth in Ti/Al diffusion couples

Diffusion couple	Range of T (°C)	Diffusion atom	n	E_a (kJ mol^{-1})	Ref.
99.7% Ti/99.7% Al (oxide layer on Ti surface suspected)	580–640	–	0.91	179.5	[7]
TiAl/Al or Ti–(5, 10, 25 wt.%)Al/Al (purity as above)	516–640	Al (sole)	0.5	94.6	[7]
Ti/Al (200 nm thin film on Si)	350–500	Ti, Al	0.5	166	[35]
OT4-1 alloy (Ti–1.0–2.5Al–1.0Mn (wt.%))/Al	530–630	Al	0.5	105.1	[8]
Ti/Al powder	750–900	–	–	517	[36]
99.99% Ti/99.99% Al	540–650	Al	0.5	34	[25]
98.7% Ti/99.2% Al (Al with 0.27% Si that goes to $TiAl_3$)	500–630	Al faster than Ti	0.5	237 ± 15	[9]
Ti–5 at.% O/Al (purity as above)	500–600	Al faster than Ti	0.5	263 ± 7	[9]
99.6% Ti/99.0% Al (75 μm foils)	650	Ti, Al	0.72	–	[5,6]
99.5% Ti/99.5% Al (175 μm foils)	525–575	Ti, Al	0.47–0.55	33.2	This work
99.5% Ti/99.5% Al (175 μm foils)	600–650	Ti, Al	0.83–1.08	295.8	This work

was reported for high-purity Ti/Al diffusion couples [25] where grain-boundary diffusion dominates.

The similar growth kinetics at 520 and 550 °C (or even slightly slower for the latter temperature) as given in Table 2 is probably related to the dominance of grain boundary diffusion at low temperatures. With increasing temperature, grain growth occurs and lattice diffusion takes a larger share. The diffusion of Ti atoms through the $TiAl_3$ lattice however is expected to be slow; the activation energy measured in the temperature range of 350–500 °C for the diffusion of Ti in $TiAl_3$ is 162 kJ mol^{-1} [35]. At a certain point during the increase of temperature it is possible that the rise in atomic flux due to increase in lattice diffusion cannot compensate for the fall due to grain growth, giving similar overall kinetics as observed in the temperature range of 520–550 °C.

A summary of reported investigations of interdiffusion of Ti/Al couples is presented in Table 4. In cases where Al was found to be the sole diffusing species and $TiAl_3$ grows towards the Ti side, the Ti side usually contains high amount of Al (e.g. [7,8]). As a result both thermodynamic and kinetic conditions for the formation of $TiAl_3$ are significantly different from those in a high purity Ti/Al couple. Likewise, many factors cause variation in the kinetic exponent and activation energy of $TiAl_3$ growth. van Loo and Rieck [7] suggested that the oxide film on Ti or Ti–Al alloys modified the growth behavior of $TiAl_3$ in such a way that a short stage of linear kinetics exists until a breakaway at which the oxide layer was broken, leaving a row of Al particles. In our method of preparing the diffusion couples, however, a layer of $TiAl_3$ about 2 μm thick was already present at the Ti/Al interfaces before the annealing started. Oxide layer on the Ti foil surfaces, if any, should have already been broken. In fact, no Al particles were observed in the $TiAl_3$ layers in the present work.

With increase in temperature to about 600 °C, a transition to a reaction-limited growth mechanism is observed in the present work (Fig. 9). Reactions at the $TiAl_3$/Al interfaces consist of two steps: (a) diffusion of Ti atoms into the Al foils until saturation; (b) nucleation of $TiAl_3$ particles. At low temperatures the first step is easily accomplished because of the very limited solubility of Ti in Al; as the temperature approaches the melting point of Al, the solubility of Ti in Al increases almost exponentially, as can be seen from a detailed investigation of the Al-rich Ti–Al phase diagram reproduced in Fig. 14 [29]. As illustrated

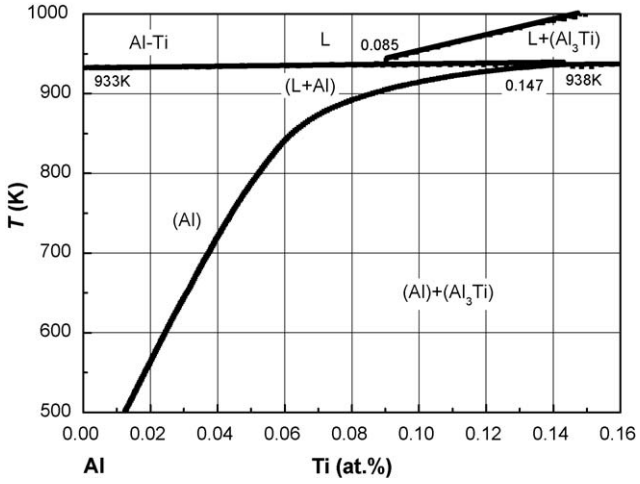

Fig. 14. Details of the Al-rich part of Al–Ti phase diagram [29].

in Fig. 13(c), for the $TiAl_3$/Al interfaces to advance a distance of δ, a critical Ti concentration, C_{Ti}, must be reached; the value of C_{Ti} increases rapidly with temperature. As a result this process of Ti diffusion in Al foils may become the limiting step of the reactions at $TiAl_3$/Al interfaces. Because of the limited solubility of Ti in Al information concerning this diffusion process is not available. However, the activation energy should be similar to that of Ti diffusion in other metals and compounds (α-Ti, Ti_3Al, TiAl, etc.), typically in the range of 250–300 kJ mol^{-1} [37]. The activation energy for the linear growth of $TiAl_3$ layers in the temperature range of 600–650 °C, 295.8 kJ mol^{-1}, is comparable to these values, suggesting that the reactions at the $TiAl_3$/Al interfaces may indeed be controlled by the diffusion of Ti atoms in the Al foils.

5. Conclusions

A systematic investigation of the growth of intermetallic $TiAl_3$ in diffusion-bonded multi-laminated Ti/Al couples has been made in the temperature range of 520–650 °C. The main conclusions are summarized as follows:

(1) In agreement with previous investigations, only $TiAl_3$ phase was detected in the Ti/Al interface zones in this work. A modified effective heat of formation model was applied to

the Ti–Al system and it predicted correctly the appearance of $TiAl_3$ as the first phase in the diffusion zone as well as subsequent formation of TiAl between Ti and $TiAl_3$ layers.

(2) Both Ti and Al are diffusing species regardless of temperature being above or below the melting point of Al. Growth of the $TiAl_3$ layers occurred mainly at the $TiAl_3$/Al interfaces.

(3) With increasing temperature there is a change in the mechanism of $TiAl_3$ growth between 575 and 600 °C from diffusion-controlled to interface reaction limited kinetics. The parabolic growth of the $TiAl_3$ layers in the low-temperature regime is dominated by grain boundary diffusion, with a low activation energy of 33.2 kJ mol^{-1}. The linear growth stage in the high-temperature regime is characterized by a high activation energy of 295.8 kJ mol^{-1}. This value is comparable to the activation energy of Ti diffusion in metals and compounds such as α-Ti, TiAl and Ti_3Al, and we assume it is also similar to the activation energy of Ti diffusion in solid Al. Based on this assumption it is suggested that the reactions at the $TiAl_3$/Al interfaces are limited by the diffusion of Ti atoms in the Al foils at the growth front of $TiAl_3$, considering the rapid increase in the solubility of Ti in Al in the high-temperature regime.

Acknowledgement

The work was partly supported by a grant from the NSFC (no. 50301014).

References

[1] D.J. Harach, K.S. Vecchio, Metall. Mater. Trans. A 32 (2000) 2001.
[2] A. Rohatgi, D.J. Harach, K.S. Vecchio, K.P. Harvey, Acta Mater. 51 (2003) 2933.
[3] L.M. Peng, J.H. Wang, H. Li, J.H. Zhao, L.H. He, Scripta Mater. 52 (2005) 243.
[4] D.J. Goda, N.L. Richards, W.F. Caley, M.C. Chaturvedi, Mater. Sci. Eng. A 334 (2002) 280.
[5] J.G. Luo, V.L. Acoff, Weld J. (Suppl.) 9 (2000) 239s.
[6] J.G. Luo, V.L. Acoff, Mater. Sci. Eng. A 379 (2004) 164.
[7] F.J.J. van Loo, G.D. Rieck, Acta Metall. 21 (1973) 61.
[8] J.M.K. Ferdinandy, D. Liška, P. Diko, Mater. Sci. Eng. A 140 (1991) 479.
[9] K. Nonaka, H. Fujii, H. Nakajima, J. Jpn. Inst. Met. 64 (2000) 85.
[10] C. Wagner, Acta Metall. 17 (1969) 99.
[11] U.R. Kattner, J.C. Lin, Y.A. Chang, Metall. Trans. A 23 (1992) 2081.
[12] J. Mackowiak, L.L. Shreir, J. Less-Comm. Met. 1 (1959) 456.
[13] J. Mackowiak, L.L. Shreir, J. Less-Comm. Met. 15 (1968) 341.
[14] A. Raman, K. Schubert, Z. Metallkd. 56 (1965) 44.
[15] U.R. Kattner, J.C. Lin, Y.A. Chang, Metall. Mater. Trans. A 23 (1992) 2081.
[16] R.M. Walser, R.W. Bené, Appl. Phys. Lett. 28 (1976) 624.
[17] B.Y. Tsaur, S.S. Lau, J.W. Mayer, M.A. Nicolet, Appl. Phys. Lett. 38 (1981) 922.
[18] R.W. Bené, Appl. Phys. Lett. 41 (1982) 529.
[19] R. Pretorius, R. de Reus, A.M. Vredenberg, F.W. Saris, Mater. Lett. 9 (1990) 494.
[20] R. Pretorius, A.M. Vredenberg, F.W. Saris, R. de Reus, J. Appl. Phys. 70 (1991) 3636.
[21] A. Laik, K. Bhanumurthy, G.B. Kale, Intermetallics 12 (2004) 69.
[22] J.L. Murray, Metall. Trans. A 19 (1988) 243.
[23] W.Y. Yang, G.C. Weatherly, J. Mater. Sci. 31 (1996) 3707.
[24] M. Thuillard, L.T. Tran, M.A. Nicolet, Thin Solid Films 166 (1988) 21.
[25] T. Shimozaki, T. Okino, M. Yamane, Y. Wakamatsu, M. Onishi, Defect Diff. Forum 143–147 (1997) 591.
[26] A.A.-H. Ahmed, Z. Metallkd. 82 (1991) 921.
[27] E. Paransky, E.Y. Gutmans, I. Gotman, M. Koczak, Metall. Mater. Trans. A 27 (1996) 2130.
[28] C.V. Ramana, B.S. Choi, R.J. Smith, R. Hutchinson, S.P. Stuk, B.S. Park, A.A. Saleh, D.R. Jeon, J. Vac. Sci. Technol. A 21 (2003) 1326.
[29] H.W. Kerr, J. Cisse, G.F. Bolling, Acta Metall. 22 (1974) 677.
[30] H.K. Kim, H.K. Liou, K.N. Tu, Appl. Phys. Lett. 66 (1995) 2337.
[31] H.K. Kim, K.N. Tu, Phys. Rev. B 53 (1996) 16027.
[32] S. Bader, W. Gust, H. Hieber, Acta Metall. 43 (1995) 329.
[33] M. Schaffer, R.A. Fournelle, J. Liang, J. Electron. Mater. 27 (1998) 1167.
[34] F.J.J. van Loo, G.D. Rieck, Acta Metall. 21 (1973) 73.
[35] J. Tardy, K.N. Tu, Phys. Rev. B 32 (1985) 2070.
[36] X. Wang, H.Y. Sohn, M.E. Schlesinger, Mater. Sci. Eng. A 186 (1994) 151.
[37] Y. Mishin, C. Herzig, Acta Mater. 8 (2000) 589.